

Retroviral infection in vivo requires an immune escape virulence factor encrypted in the envelope protein of oncoretroviruses

Géraldine Schlecht-Louf^{a,b,1}, Martial Renard^{a,1}, Marianne Mangeney^{a,1}, Claire Letzelter^a, Aurélien Richaud^a, Bertrand Ducos^a, Isabelle Bouallaga^a, and Thierry Heidmann^{a,2}

^aUnité des Rétrovirus Endogènes et Éléments Rétroïdes des Eucaryotes Supérieurs, Centre National de la Recherche Scientifique, Unité Mixte de Recherche 8122 Institut Gustave Roussy, 94805 Villejuif, and Université Paris-Sud, 91405 Orsay, France; and ^bFaculté de Médecine Paris-Sud, Université Paris-Sud, 94276 Le Kremlin-Bicêtre cedex, France

Edited* by John M. Coffin, Tufts University School of Medicine, Boston, MA, and approved January 6, 2010 (received for review November 13, 2009)

We previously delineated a highly conserved immunosuppressive (IS) domain within murine and primate retroviral envelope proteins (Envs). The envelope-mediated immunosuppression was manifested by the ability of the proteins, when expressed by allogeneic tumor cells normally rejected by engrafted mice, to allow these cells to escape, at least transiently, immune rejection. Using this approach, we identified key residues whose mutation specifically abolishes IS activity without affecting the “mechanical” fusogenic function of the entire envelope. Here, we genetically “switched off” the envelope-mediated immunosuppression of an infectious retrovirus, the Friend murine leukemia virus, while preserving mutant envelope infectivity both *ex vivo* and *in vivo*, thus allowing us to test the functional importance of envelope-mediated immunosuppression in retrovirus physiology. Remarkably, we show, *in vivo*, that the non-IS mutant virus displays the same propagation kinetics as its WT counterpart in irradiated immunocompromised mice but that it is rapidly and totally cleared from normal immunocompetent mice, which become fully protected against a challenge with the WT retrovirus. Using cell depletion strategies, we further establish that envelope-mediated immunosuppression enables the retrovirus to escape innate (natural killer cells) and adaptive (CD8 T cells) antiviral effectors. Finally, we show that inactivated mutant virions induce higher humoral and cellular responses than their WT counterparts. In conclusion, our work demonstrates the critical role of Env-induced immunosuppression for retrovirus propagation *in vivo* and identifies a unique definite target for antiretroviral therapies and vaccine strategies, also characterized in the human T-cell leukemia virus (HTLV) and xenotropic murine leukemia virus-related virus (XMRV) retroviruses, opening unprecedented prospects for the treatment of retroviral diseases.

infectious retrovirus | immunosuppression | innate immunity | adaptive immunity | vaccination

As both clinical and experimental data have shown, most viruses have adapted to prevent their rejection by the host immune system during acute infection, to an extent sometimes resulting in the establishment of persistent infections (1–4). Persistent viruses, and notably retroviruses, have developed diverse strategies to subvert the host antiviral response, which allow them to escape the innate and adaptive immune system by directly affecting and/or inducing specific sets of immune cells, including natural killer (NK), CD8 T, or regulatory T (Treg) cells (5, 6). To characterize, and possibly counteract, the mechanisms by which retroviruses escape immune rejection, we thought that identification of the viral effector protein(s) associated with this activity would be an unavoidable prerequisite.

An immunosuppressive (IS) activity of retroviral envelope proteins (Envs) was initially reported *ex vivo* (7) and further substantiated in our group using an *in vivo* tumor rejection assay (8–10). In this model, we showed that the full-length Env of Moloney murine leukemia virus (Mo-MLV), as well as its transmembrane (TM) subunit alone, is immunosuppressive (9), and further

delineated a highly conserved immunosuppressive domain (ISD) within retroviral Envs (10). However, the importance of this IS function for infectious retrovirus propagation *in vivo* remained unknown. To answer this question, we (*i*) looked for a murine retrovirus whose viremia could be easily monitored *in vivo* and (*ii*) attempted to introduce appropriate mutations into a cloned element so as to knock out the IS activity of the viral Env specifically without altering its fusogenic properties or the overall replicative properties of the retrovirus in *ex vivo* assays or in immunocompromised mice.

The Friend virus is a complex of mouse retroviruses composed of the nonpathogenic replication-competent Friend murine leukemia virus (F-MLV) and a pathogenic replication-defective spleen focus-forming virus (SFFV). An F-MLV provirus has been cloned (11), making possible *ex vivo* production of N-tropic infectious particles as well as introduction of definite mutations within the viral sequence by genetic engineering. F-MLV was therefore selected as a suitable model for the present *in vivo* studies.

In our previous work on the ISD of the captured endogenous retroviral syncytin proteins (10), and because of the unexpected characteristic of one of them (syncytin-1), which has lost its IS activity but has fully conserved its “mechanical” fusogenic activity, we were able to identify, within the ISD, definite amino acids that govern IS activity as well as specific amino acid substitutions that allowed its switching on and off without altering the fusogenicity of the mutated Envs. Because of the incredibly high structure conservation within the ectodomains of retroviral Envs (12), we have here attempted to generate a mutant F-MLV deprived of IS activity by following the same rules. This led us to construct an F-MLV immunosuppression-negative mutant, with infectious capacity indistinguishable from that of the WT virus *in vitro*. This mutant allowed us to demonstrate unambiguously that (*i*) a functional ISD is absolutely required for viremia *in vivo* in immunocompetent mice, (*ii*) the ISD inhibits both the innate and adaptive arms of the immune response, and (*iii*) the mutations within the ISD resulting in loss of its IS activity are associated with enhanced immunogenicity of the viral antigens. We also identified functional ISDs in other retroviruses, namely, the human T-cell leukemia virus (HTLV) and the xenotropic murine leukemia virus-related virus (XMRV) initially discovered in human prostate tumors (13), which therefore become, according to the

Author contributions: G.S.-L., M.R., M.M., and T.H. designed research; G.S.-L., M.R., M.M., C.L., A.R., B.D., and I.B. performed research; G.S.-L., M.R., M.M., and T.H. analyzed data; and G.S.-L., M.R., M.M., and T.H. wrote the paper.

The authors declare no conflict of interest.

*This Direct Submission article had a prearranged editor.

¹G.S.-L., M.R., and M.M. contributed equally to this work.

²To whom correspondence should be addressed. E-mail: heidmann@igr.fr.

This article contains supporting information online at www.pnas.org/cgi/content/full/0913122107/DCSupplemental.

present mouse model and experimental results, definite targets for therapeutical antiviral approaches as well as optimized vaccine antigens when adequately mutated.

Results

Generation of a Mutant, Immunosuppression-Negative, Functional F-MLV. As illustrated in Fig. 1A, the MLV retroviral Env comprises within its TM subunit a sequence that we have previously delineated as responsible for its IS activity. The 20-aa sequence shown in Fig. 1A corresponds to that of both Mo-MLV and F-MLV. Despite significant divergence between the primary sequence of the 20-aa ISD of MLV Env and that of the previously characterized syncytin-1 and Mason–Pfizer monkey virus (MPMV) Env, we reasoned that the high 3D structure conservation of ISDs (10, 12) should allow direct identification of the amino acids involved in IS activity as well as the substitutions required for specific loss of IS function within the MLV ISD. Accordingly, we replaced the key E14 and A20 residues of the F-MLV Env ISD with those of the non-IS syncytin-1, namely, R14 and F20 (Fig. 1A), as described in our previous work (10), and checked whether it would affect the infectivity of Env pseudotypes (Fig. 1B). As previously described for MPMV Env (10), the single mutation of one or the other of these two key residues altered infectivity, although not to the same extent, but the double mutation did not, showing that combining the E14R and A20F mutations in the double mutant (DM) fully restores infectivity to WT level.

The IS property of DM F-MLV Env was then analyzed using the *in vivo* tumor rejection assay that we had previously used to demonstrate IS activity of the Mo-MLV and MPMV Envs as well as that of the Mo-MLV TM subunit alone (8–10). The rationale of the assay has been previously described (9, 10) and can be summarized as follows: Whereas injection of MCA205 tumor cells (H-2^b) into allogeneic BALB/c mice (H-2^d) leads to the formation of no tumor or transient tumors that are rapidly rejected, injection of the same cells stably expressing an IS retroviral Env leads to the growth of larger tumors that persist for a longer time in spite of

the expression of the exogenous antigen. This difference is not associated with a difference in intrinsic cell growth rate because it is not observed in syngeneic C57BL/6 mice and is dependent on the immune system (9, 10). The extent of “immunosuppression” can be quantified by an index based on tumor size, with a positive index indicating that *env* expression facilitates tumor growth as a consequence of its IS activity and a null or negative index pointing to no effect or even enhanced rejection, respectively (the latter may be explained by stimulation of the immune response of the host against the foreign antigen, represented by a non-IS Env expressed at the surface of the tumor cells). As illustrated in Fig. 1C, and as expected from the 100% sequence identity between the Mo-MLV and F-MLV ISDs, F-MLV Env is immunosuppression-positive, and, remarkably, the doubly mutated but still functional Env becomes immunosuppression-negative.

We then replaced the WT *env* gene by its non-IS DM counterpart in the F-MLV proviral molecular clone 57 (11) and produced *ex vivo* each type of retroviral particle. Viral particles were generated on transfection of 293T cells with the WT or DM p57 plasmid and infection of NIH/3T3 producer cells with the harvested cell supernatant. Virus yields for either plasmid were similar, as measured by a quantitative RT-PCR assay of viral RNA in the NIH/3T3 producer cell supernatants. Furthermore, both viruses displayed the same propagation kinetics in an *in vitro* infection assay in NIH/3T3 cells (Fig. 1D; see also Fig. S1 for Internal Ribosome Entry Site (IRES)-*gfp*-marked viruses), confirming that F-MLV DM Env is fully functional and that the introduced mutations have no effect on viral replication.

Requirement of Env Immunosuppressive Function for Viral Spread *In Vivo*. To assess the role of Env-induced immunosuppression during retroviral infection, we compared the *in vivo* propagation of WT and DM F-MLV by quantifying viral loads in mouse serum. This work was carried out using Swiss mice, which were selected because (i) they are highly sensitive to infection with the N-tropic F-MLV and (ii) as noncongenic outbred animals, they constitute a more “real-life” model host than any inbred mouse strain. In this model, as illustrated in Fig. 2A, WT F-MLV first caused a high viremia in all animals during the primary infection phase (peak at day 7 after virus injection), followed by the establishment of a persistent infection with viremia reaching a plateau. In contrast, the non-IS DM F-MLV was absent (or barely detectable in 4 of 10 mice) at day 7 and undetectable 14 days after injection (as similarly observed when using even higher doses of virus; see Fig. 4). Importantly, mice immunocompromised by 5-Gy x-ray irradiation before infection displayed similar viral loads when injected with either WT or DM F-MLV, at least during the first 2 weeks of infection (Fig. 2B), thus excluding the possibility that DM F-MLV is deficient in any step of its *in vivo* replication, consistent with the *in vitro* data (Fig. 1B and D). However, DM F-MLV was eliminated when the mouse immune system recovered from irradiation, with no more viremia detected 4 weeks postinfection. These experiments thus demonstrate that retroviral Env is not solely a mechanical component of the viral particle driving entry into target cells but is also a critical effector in the host–parasite relationships essential for MLV infection.

Role of NK Cells in Virus Control. To understand the mechanism involved in the ISD-dependent viral escape from the host immune system, we searched for immune effectors responsible for rejection of the mutant F-MLV, reasoning that because these effectors were not able to eliminate WT F-MLV, they should be, directly or indirectly, the target of Env-driven immunosuppression. Because of the rapid “control” of DM F-MLV (Fig. 2A), we suspected a role for innate immune effectors, and therefore tested the possible involvement of NK cells, known for their antiviral activity, on *in vivo* cell depletion. Because not all the animals from the outbred Swiss mouse strain were found to express the NK1.1 antigen, a

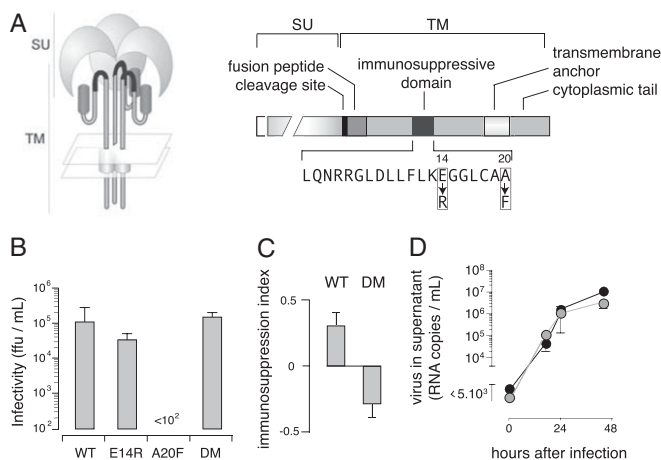


Fig. 1. Characterization of the fusogenic and IS activities of F-MLV Env and generation of a fusion-positive immunosuppression-negative specific mutant. (A) Schematic representation of the F-MLV Env with the surface (SU) and TM subunits, the furin cleavage site, the hydrophobic fusion peptide, the TM anchor, and the IS domain with its peptide sequence indicated; the E > R and A > F substitutions generated in the single mutant or DM are positioned. (B) Infectivity of Mo-MLV virions pseudotyped with F-MLV Env, WT, single mutants (E14R, A20F), or DM. Infectivity is measured using NIH/3T3 cells as target cells and is expressed as LacZ⁺ focus-forming units (ffu)/mL supernatant (mean ± SD, *n* = 3). (C) *In vivo* IS activity of WT and DM F-MLV Env. IS activity is assayed using F-MLV *env*-transduced MCA205 tumor cells engrafted into allogeneic BALB/c mice and is quantified by an index based on tumor size (mean ± SD, *n* = 3) (10). (D) Compared *in vitro* propagation rates of WT (black circles) and DM (gray circles) F-MLV virions using NIH/3T3 cells as target cells. Viral loads in supernatants are measured by quantitative RT-PCR (mean ± SD, *n* = 4).

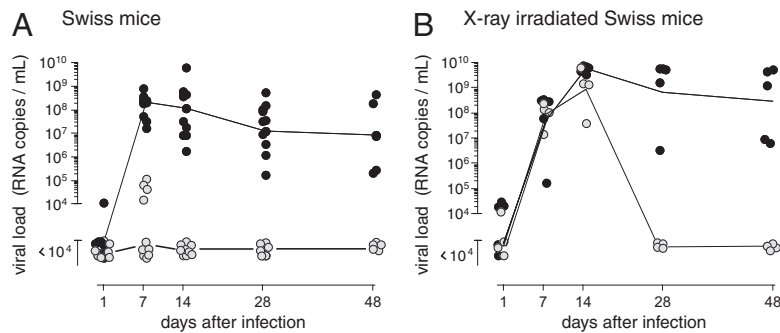


Fig. 2. An immunosuppression-positive domain is required for F-MLV propagation in immunocompetent mice. Viremia of untreated (A) or x-ray-irradiated (B) Swiss mice on infection with WT (black circles) or the non-IS DM (gray circles) F-MLV. Mice were i.v. injected at day 0, and viral loads were measured by quantitative RT-PCR from blood samples collected at the indicated times (viral RNA copies/mL). In B, mice were x-ray-irradiated (5 Gy) 2 days before infection. Each circle corresponds to one individual mouse, with the lines connecting the geometric means. No viral RNA was detected in PBS-injected control mice.

surface marker specific for NK and natural killer T (NKT) cells in certain mouse strains, NK1.1⁺ mice were first sorted based on their blood cell NK1.1 expression before being treated with the anti-NK1.1 antibody. As shown in Fig. 3A, NK1.1⁺ cell depletion enabled the propagation of DM F-MLV, with viral loads similar to those observed with WT F-MLV when assayed 5 days postinfection. As a control, this effect was not observed on treatment of NK1.1⁻ Swiss mice by the anti-NK1.1 antibody, with no viremia detected for DM F-MLV (Fig. S2). Accordingly, an NK1.1⁺ cell subset, most probably NK cells, efficiently and rapidly eliminates DM F-MLV but fails to block WT virus. However, propagation of DM F-MLV in the antibody-treated mice was transient, and the virus was completely eliminated by 7 days after infection, despite maintenance of the NK-depleted state. This observation indicates that a second mechanism for virus clearance, independent of the NK1.1⁺ cells, takes over at a later time to eradicate the mutant virus, with kinetics compatible with the establishment of adaptive immunity.

Role of Cytotoxic T Lymphocytes in Virus Control. To demonstrate the role of the adaptive immune response in the second phase of mutant F-MLV elimination, we used athymic Swiss-Nude mice. As observed above, depletion of the NK1.1⁺ cell subset first allowed

the propagation of DM F-MLV, to the same extent as WT F-MLV (Fig. 3B). This time, however, DM F-MLV viremia persisted as long as NK cell depletion was maintained, consistent with the virus rejection observed in normal mice in the absence of NK cells (Fig. 3A) being driven by the adaptive immune system. Incidentally, this experiment also shows that the NK1.1⁺ cells responsible for early rejection of DM F-MLV are NK cells and not NKT cells, because the latter require the thymus to differentiate (14). These results demonstrate that NK cells, per se, are sufficient to eradicate non-IS F-MLV both at the early stage of infection and also at a later stage when the virus is then additionally cleared by a T-cell-dependent mechanism.

To characterize further the latter process and the likely involvement of CD8 T cells, we again used depleting antibodies directed against the CD8 α -cell surface marker, which led to CD8 T-cell elimination (Fig. 3C). In Swiss mice simultaneously depleted for NK and CD8 T cells, DM F-MLV persisted in the serum as long as the treatment lasted, whereas it was not detected at any time in mice only treated with the anti-CD8 antibodies (Fig. 3C) or with a control antibody. Thus, IS activity of the WT F-MLV Env allows the virus to escape two types of antiviral, NK cell-dependent and CD8 T-cell-dependent, immune activity.

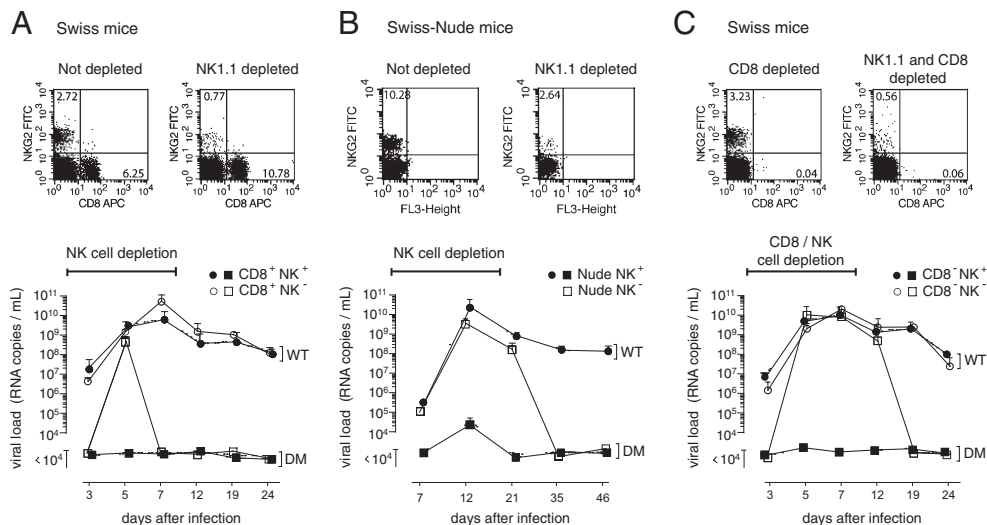


Fig. 3. Cellular targets of the Env-mediated immunosuppression effect assayed by immune cell depletions *in vivo*. Serum viral loads (Lower) after injection of WT (○ and ●) or DM (□ and ■) F-MLV were measured in untreated (● and ■) or NK1.1-depleted (○ and □) Swiss (A) or Swiss-Nude (B) mice or in CD8-depleted (● and ■) or CD8-depleted plus NK1.1-depleted (○ and □) Swiss mice (C). The data correspond to the mean \pm SD for five mice and are representative of two to seven independent experiments. Cell depletions (duration of antibody treatment indicated with a bar; *Materials and Methods*) were controlled by flow cytometry on blood samples (Upper), with numbers in the dot plot corners indicating the percentage of labeled cells in the corresponding quadrant. NK cell recovery after the last antibody injection was 50% 5 days later and >90% at day 8.

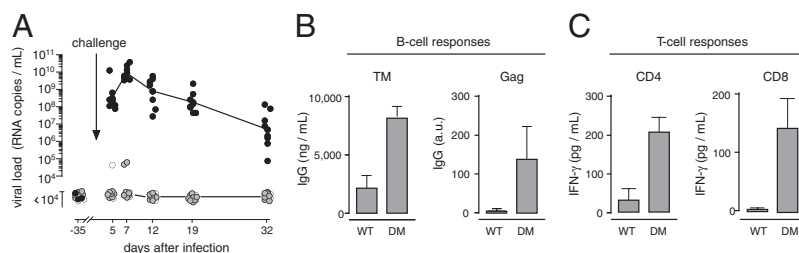


Fig. 4. Mutation within the F-MLV ISD confers protective activity and enhances immunogenicity. (A) Protection of mice immunized with DM F-MLV and challenged with WT F-MLV. Swiss mice were injected with 8×10^8 RNA copies of DM F-MLV (white and gray circles) or with PBS (black circles), and the absence of viremia was checked 4 weeks later (day -35). Nine weeks after infection, mice were challenged with 4×10^7 RNA copies of WT F-MLV (gray and black circles) or injected with PBS (white circles), and postchallenge sera samples were collected at the indicated time points. Each circle corresponds to one individual mouse, with the lines connecting the geometric means of eight mice; data are representative of more than three independent experiments, with no significant departure from full control of viremia by the vaccinated mice in all cases. (B and C) Compared immunogenicity of WT and DM UV-inactivated F-MLV. C57BL/6 mice were injected three times with a 1-week interval with 10^9 RNA copies of UV-inactivated WT or DM F-MLV in the presence of $50 \mu\text{g}$ of CpG ODN. (B) One week after the last injection, mice were blood-sampled and serially diluted serum was used to detect TM-specific (Left) and Gag-specific (Right) IgG by ELISA. Results are the mean \pm SD of five mice and are representative of three independent experiments. (C) Ten days after the last injection, mice were killed and splenocytes were restimulated in vitro for 72 h in the presence or absence of the I-A^b-restricted H19 Env peptide (Left) or K^b-restricted Gag peptide (Right). Specific IFN- γ secretion by CD4 or CD8 T cells was detected in culture supernatants by standardized sandwich ELISA. Data are the mean \pm SD of three independent experiments performed with three to four mice per group.

Of note, a similar depletion procedure applied to CD25⁺ cells (thus including the natural Treg cells) before F-MLV infection had no effect on WT F-MLV viremia in vivo and, as expected, did not allow DM F-MLV to propagate (Fig. S3 and Discussion).

Protective Activity and Immunogenicity of the Mutant F-MLV. The data in Figs. 2 and 3 clearly show that the mutant immunosuppression-negative F-MLV, does not propagate in immunocompetent mice and, as such, behaves as a bona fide live-attenuated virus. To determine whether it could act as a vaccine, a series of Swiss mice were first injected with DM F-MLV; the absence of viremia was checked 4 weeks postinfection, and mice were finally challenged with WT F-MLV. As shown in Fig. 4A, all the “vaccinated” mice were protected against challenge, with none of them developing significant viremia under conditions in which all mock-vaccinated (with PBS) mice became viremic. Clearly, the mutant virus has generated protective immunity against WT F-MLV. Of note, attempts to detect virus-specific T-cell responses by IFN- γ ELISpot were not successful. Furthermore, antibodies against F-MLV Env and Gag proteins were detected in the serum of the vaccinated mice, but IgG levels were low (twice the background level, as shown in Fig. S4A–C), with no detectable neutralizing activity (Fig. S4D). Clearly, as similarly observed for other retroviruses and animal models (15, 16), the protective immunity induced by the attenuated F-MLV is not associated with high immune responses.

To characterize further the immune response induced by the immunosuppression-negative DM F-MLV, under well-defined conditions, we chose to inject UV-inactivated F-MLV in inbred C57BL/6 mice to (i) work with the same amounts of antigen for WT or DM F-MLV and (ii) analyze specific T-cell responses against well-defined immunodominant H-2^b-restricted antigenic peptides (17, 18). As shown in Fig. 4, both humoral and cellular virus-specific responses could be detected, although they were still found to be very low. Interestingly, Fig. 4 also shows that injection of the immunosuppression-negative DM F-MLV reproducibly induced significantly higher responses than its WT counterparts for both anti-TM and anti-Gag IgG as well as for IFN- γ secretion by CD4 and CD8 T cells, suggesting that Env-mediated immunosuppression impairs, at least quantitatively, the induction of antiviral responses. This inhibitory effect was still observed when recombinant proteins of only 64 aa, corresponding to the Env ectodomains, were injected: A 40-fold increase in the IgG response was detected in the case of DM vs. WT F-MLV ectodomain injection (Fig. S5). A large increase was also observed for

the TM ectodomains mutated along the same rules for the closely related recently identified human XMRV retrovirus (13) as well as for the HTLV retrovirus (Fig. S5). These results indicate that mutation of the retroviral ISD could be useful to improve viral antigen immunogenicity for future vaccine strategies.

Discussion

Thus far, the physiological role of retroviral Env immunosuppressive function has remained elusive. In the current study, we succeeded in “switching off” the IS function of F-MLV Env without altering its fusogenic activity by replacing two specific amino acids in its TM subunit according to the rule that we had previously established for other retroviral Envs (10). Although the ISD overlaps the very constrained helix-loop-helix segment of the Env TM ectodomain that is believed to play a pivotal role in its conformational changes during the fusion process, this double mutation preserved its mechanical fusogenic function in a series of in vitro infectivity assays, including infectivity of pseudotypes, and replication efficiency of reconstructed mutant F-MLV proviruses. Indeed, the immunosuppression-negative DM F-MLV Env could be introduced back into the complete F-MLV cloned provirus, resulting in a mutant F-MLV retrovirus that disclosed infectivity and replication efficiency in vitro identical to that of WT virus, as assayed on NIH/3T3 cells with either the “basic” virus or an IRES-*gfp*-marked version of the virus. Full conservation of the functionality of DM F-MLV was further ascertained by the in vivo infection assay performed on immunocompromised x-ray-irradiated mice, which disclosed viremia identical to that of the WT virus, at least in the initial stages of infection. Thanks to the achieved genetic disjunction between the Env fusogenic and IS activities, the physiological impact of the IS function carried by a retroviral Env could then be unambiguously and specifically determined. Remarkably, we could demonstrate that the immunosuppression-negative DM F-MLV is unable to propagate in untreated immunocompetent mice under conditions in which such mice become persistently infected by WT F-MLV. Again, lack of viral propagation of DM F-MLV in vivo is not dependent on some mechanical defect of the virus but actually depends on loss of the Env-associated IS function, with viremia being indistinguishable from that of WT virus in the irradiated mice assayed in parallel. These conclusions are further strengthened by the specific NK and/or CD8 T-cell depletion experiments that were carried out with DM F-MLV, which resulted in recovery of viral loads as high as those observed with WT F-MLV at varying stages of infection, consistent again with full intrinsic replicative

“competence” of the mutant virus but with involvement of a viral-associated “immune” activity restricted to the WT virus. Clearly, retroviral Envs are not solely a “mechanical component” of the viral particle driving entry into the target cell but are also a critical immunological “cytokinal” effector in the host–parasite relationships, absolutely required for viral spread.

Another important outcome of the study is the identification of a dual immune activity of the viral ISD. Indeed, we show that when F-MLV is deprived of its IS function, NK cells alone can efficiently prevent primary infection (Fig. 3B and C) and even decrease viral loads to undetectable levels in case of an established viremia (Fig. 3B), whereas they fail to do so with the WT virus. On the other hand, CD8 T cells alone also prove to be sufficient to eliminate the mutant virus even when the viral load has reached high levels (Fig. 3A), whereas, again, they fail to do so with the WT virus. Altogether, these experiments show that both the innate (NK cells) and adaptive (CD8 T cells) immune systems are able to prevent *in vivo* spread as well as persistence of the non-IS mutant F-MLV and that they are both, directly or indirectly, inhibited by the ISD of the WT immunosuppression-positive F-MLV.

The precise mechanism by which the now clearly identified retroviral IS function inhibits the innate and adaptive antiviral immune responses at the molecular level is still largely unknown, but a series of putative cellular mediators can be inferred. Among them, Treg cells are known to suppress both CD8 T-cell and NK cell function (19, 20) and have been implicated by several researchers in retroviral invasion and persistence (6, 21). Several studies have shown impairment of virus-specific CD8 T-cell responses by Treg cells in chronic infection by the F-MLV/SFFV complex (22–27), which could thus be activated and/or induced by the F-MLV Env-associated IS activity. However, the cell depletion experiments that we carried out to eliminate CD25⁺ natural Treg cells during the early phase of F-MLV infection had no effect on viremia, excluding a pivotal role of these cells. Other studies using the F-MLV/SFFV complex have also shown that Treg cell inhibition or depletion is not sufficient for virus elimination (26–28). Thus, Treg cells, either natural or induced, are most probably not primary effectors of Env-mediated immunosuppression. Dendritic cells (DCs) are also known to be essential for both NK cell activation and CD8 T-cell priming (29, 30), and they are good candidates for being involved in the control of F-MLV *in vivo*. Further work is required to determine whether DC functions (e.g., migration, cytokine secretion) are altered, and possibly differentially affected, by F-MLV in its WT and immunosuppression-negative versions.

Whatever the mechanism underlying Env-mediated immunosuppression, the present investigation has another important outcome because it suggests a simple method for improving antiviral vaccines. Indeed, in addition to identifying a target for antiretroviral strategies, we provide evidence that inhibition of ISD activity, through appropriate mutations, significantly improves immunogenicity of both recombinant Envs and inactivated virions. Indeed, with the immunosuppression-negative mutants, we observed a significant increase in both the B- and T-cell responses against antigenic determinants carried by the viral Env and Gag proteins. Because the mutation strategy we devised minimally alters antigenicity, with only two amino acids being mutated within the whole viral proteins and with the structure and fusion function of the mutated Env being unaltered, it is likely that the increased immunogenicity of the mutant “optimized” antigens results from the abolition of the IS activity naturally carried along with them. If general, this finding could provide a way to dramatically improve currently unsatisfactory vaccination attempts directed against retroviruses, including those pathogenic in humans.

Along this line, the results presented for the HTLV and XMRV retroviruses (Fig. S5), disclosing a very significant increase in B-cell responses following introduction of specific mutations in

their identified ISD associated with the inhibition of their IS activity, should augur well for the proposed vaccine strategy.

Materials and Methods

Mice and Cells. Swiss (N-tropic F-MLV permissive), BALB/c, and C57BL/6 mice, aged 6–10 weeks old, were obtained from Janvier. Swiss-Nude mice were obtained from the Institut Gustave Roussy breeding center. 293T (CRL11268), HeLa (CCL2), NIH/3T3 (CRL-1658), and MCA205 cells (31) were cultured in DMEM with 10% (vol/vol) FCS, streptomycin (100 µg/mL), and penicillin (100 U/mL). Mouse splenocytes were cultured in RPMI with 10% (vol/vol) FCS, antibiotics as above and 5×10^{-5} M β -mercaptoethanol.

Plasmids. pHCMV-envF-MLV was constructed by inserting the F-MLV *env* gene retrieved by PCR from p57 (gift from M. Mougé, UMR5236, Montpellier, France) (11) using primers 1 and 2 (primer sequences are provided in *SI Text*) and digested with XhoI and MluI, into pHCMV-env HERV-T (32), which was digested with the same enzymes. Each mutant derivative was constructed by a three-fragment ligation of pHCMV-envF-MLV opened by ClaI/AvrII, and two PCR products generated with primer pairs 3–4 and 5–6 (Table S1) for the E14R mutation, primer pairs 3–7 and 6–8 for the A20F mutation, and primer pairs 2–3 and 6–8 for the E14R + A20F mutation, restricted with ClaI and AvrII. The p57 DM F-MLV was constructed by inserting the BstZ111/BsmI fragment of the pHCMV-envF-MLV DM into p57 digested with the same enzymes. The pDFG retroviral vector expressing the WT or DM F-MLV Env (and hygromycin resistance) for stable transduction of MCA205 cells was constructed by inserting the BspEI/MluI fragment from pHCMV-envF-MLV into pDFG-MoTM1 (10) digested with AgeI/MluI. The bacterial expression vectors for WT and DM F-MLV Env ectodomains were constructed by inserting a PCR fragment, generated with WT or DM pHCMV-envF-MLV as a template and primers 9 and 10 and digested with NcoI/XhoI, into pET28⁺b (Novagen) digested with the same enzymes.

Infectivity Assay with Pseudotyped Virions. Mo-MLV virions pseudotyped with WT or DM F-MLV Env were produced as described by Blaise et al. (33) by cotransfecting 7.5×10^5 293T cells with 0.55 µg of pHCMV-envF-MLV, 1.75 µg of a Mo-MLV *gag-pol* vector (33), and 1.75 µg of a LacZ-marked defective retroviral vector (pMFGsnls/lacZ), using calcium phosphate precipitation (Invitrogen). Thirty-six hours after transfection, viral supernatants were harvested and filtered through 0.45-µm pore-sized membranes; 5–500 µL of supernatant supplemented with 8 µg of polybrene per milliliter was transferred onto NIH/3T3 target cells (seeded in 24-well plates at 10^4 cells per well the day before infection). Viral titers were measured by X-Gal staining 3 days postinfection and expressed as lacZ focus-forming units/mL of viral supernatant.

In Vivo Tumor Rejection Assays. The assay was performed as described by Mangeney et al. (10). Briefly, MLV virions containing the WT or DM F-MLV *env*-expressing pDFG retroviral vector described above were produced by transfecting 293T cells with 1.75 µg of the pDFG vector plus nonretroviral expression vectors for the MLV proteins [0.55 µg for MLV *env* and 1.75 µg for MLV *gag-pol* (33)]. Released particles were then used to transduce MCA205 cells (5×10^5 cells). Cells were cultured in selective medium (400 U/mL hygromycin) for 3 weeks and finally scraped without trypsin to be inoculated *s.c.* into the mouse flank as described by Mangeney and Heidmann (9). Tumor area (mm²) was determined by measuring perpendicular tumor diameters three times weekly, and extent of immunosuppression was quantified by an index based on tumor size ($A_{env} - A_{none}$)/ A_{none} , where A_{env} and A_{none} are the mean areas at the peak of growth of tumors from mice injected with *env*-expressing or control cells, respectively.

F-MLV Production and Assay. A total of 7.5×10^5 293T cells were transfected with 4 µg of WT or DM p57 DNA using calcium phosphate transfection (Invitrogen). Cell supernatants were collected 48 h later, filtered through 0.45-µm pore-sized membranes, supplemented with 8 µg/mL polybrene, and used to infect 5×10^5 NIH/3T3 cells. Infected cells were cultured for 4 additional days and expanded, and supernatants were collected from days 4 to 8 postinfection. Viral particles were concentrated by ultracentrifugation, resuspended in PBS, and frozen for further use. Viral RNA (from 2 µL of concentrated virus, 20 µL of cell supernatant, or 20 µL of mouse serum) was extracted using the RNeasy microkit (QIAGEN) and reverse-transcribed using the Mo-MLV RT kit (Applied Biosystems) with random hexamers as primers, and the cDNA was quantified by real-time PCR using the Platinum SYBR Green qPCR kit (Invitrogen) and primers CTCAGGGAGCAGCGGA and TAGCTAAGTCTGTCCAGGCAGTG. Only values $>10^4$ RNA copies/mL are significant.

In vitro replication of WT and DM F-MLV was assayed on infection of 10^4 NIH/3T3 cells (in six-well plates) with 10^7 viral copies, supernatants were collected,

and viral loads were measured as described previously over a 3-day period. In vivo replication of WT and DM F-MLV was assayed on infection of Swiss or Swiss-Nude mice by i.v. injection of 10^7 viral copies in PBS and viral loads measured in blood samples (retroorbital bleed). UV-inactivated WT and DM F-MLV virions were obtained by irradiation under the cell culture hood at $5 \times 10^5 \mu\text{J}/\text{cm}^2$.

Immune Cell Depletions. PK136, YTS169, and PC61 hybridomas producing depleting antibodies against the NK1.1, CD8 α , and CD25 antigens, respectively, were obtained from L. Zitvogel. Ascites were produced in nude mice, and antibodies were purified by FPLC using protein A columns. NK cell depletions were performed by i.p. injection of 300 μg of anti-NK1.1 antibodies on days -3, 0, 3, 7, and 10 postinfection for Swiss mice. For nude mice, two additional injections were performed at days 13 and 17. CD8 T-cell depletions were performed by injecting 100 μg of anti-CD8 antibodies at days -1, 0, 5, and 10 postinfection. CD25 depletions were performed by i.p. injection of 100 μg of anti-CD25 antibodies the day before infection. Depletions were checked at day 5 postinfection by quantifying NK, CD8, and CD25 cells in mouse blood by flow cytometry, using the 20d5 anti-NKG2A/C/E (Serotec), 53-6.7 anti-CD8 (Miltenyi Biotec), and 3C7 anti-CD25 (BD Biosciences) antibodies, respectively.

Recombinant Proteins, Peptides, and Oligonucleotides. Recombinant proteins were produced as described by Mangeney et al. (10) using BL21 (DE3) *Escherichia coli* cells (Stratagene) and pET28⁺-derived expression vectors (as described above). Recombinant WT and DM TM subunit ectodomains and Gag protein were soluble and were purified on HiTrap Chelating HP columns (Amersham). WT and DM ectodomains were further purified through a Superdex 75 HR10/30 column (Amersham) to isolate the major trimeric form. The synthetic Gag_{L85-93} (CCLCLTVFL) peptide corresponding to the immunodominant D^b-restricted CD8⁺ T-cell epitope from F-MLV Gag (17) and the

synthetic H19-Env₁₂₂₋₁₄₁ (EPLTSLTPRCNTAWNRLKL) peptide corresponding to the immunodominant I-A^b-restricted CD4⁺ T-cell epitope from F-MLV gp70 (18) were obtained from Sequentia. CpG oligonucleotide (TCCATGAC-GTTCTGACGTT) and control (TCCAGGACTTCTCTCAGGTT) were synthesized by Prologo.

Anti-F-MLV Antibody Detection and IFN- γ Assay. IgG levels in serially diluted mouse sera were assayed by indirect ELISA using MaxiSorp microplates (Nunc) coated with recombinant Gag or TM subunit ectodomains (2 $\mu\text{g}/\text{mL}$), anti-mouse IgG antibodies conjugated to HRP (Amersham), and a BD-Opteia revelation kit (Sigma). Mouse anti-His₅ antibody (QIAgen) was used for standardization. Splenocytes from immunized mice were stimulated in vitro with or without 10 $\mu\text{g}/\text{mL}$ Gag_{L85-93} or H19-Env₁₂₂₋₁₄₁ peptide, and the supernatants were harvested 72 h later. IFN- γ production was then measured by sandwich ELISA, using MaxiSorp plates coated with an unconjugated anti-IFN- γ antibody (R4-6A2; BD Biosciences) and detection with a biotinylated antibody (XMG1.2; BD Biosciences). Plates were developed using streptavidin-HRP (BD Biosciences) and o-phenylenediamine (Sigma-Aldrich) and standardized using murine recombinant IFN- γ (BD Biosciences). IFN- γ levels are given after subtracting nonspecific IFN- γ secretion in the absence of stimulating peptides.

ACKNOWLEDGMENTS. We thank Laurence Zitvogel for giving us the PK136 and YTS169 hybridomas; Benoit Salomon for the PC61 hybridoma, and Marylene Mougel for the p57 plasmid, as well as the Service Commun d'Expérimentation Animale (Institut Gustave Roussy) for animal care. We thank Christian Lavialle for comments and critical reading of the manuscript. This work was supported by grants from the Centre National de la Recherche Scientifique and Ligue Nationale contre le Cancer (équipe labellisée).

- Bowie AG, Unterholzner L (2008) Viral evasion and subversion of pattern-recognition receptor signalling. *Nat Rev Immunol* 8:911-922.
- Hansen TH, Bouvier M (2009) MHC class I antigen presentation: Learning from viral evasion strategies. *Nat Rev Immunol* 9:503-513.
- Jonjić S, Babić M, Polić B, Krmpotić A (2008) Immune evasion of natural killer cells by viruses. *Curr Opin Immunol* 20:30-38.
- Malim MH, Emerman M (2008) HIV-1 accessory proteins—Ensuring viral survival in a hostile environment. *Cell Host Microbe* 3:388-398.
- Iannello A, et al. (2006) Viral strategies for evading antiviral cellular immune responses of the host. *J Leukocyte Biol* 79:16-35.
- Schneider-Schaulies S, Dittmer U (2006) Silencing T cells or T-cell silencing: Concepts in virus-induced immunosuppression. *J Gen Virol* 87:1423-1438.
- Cianciolo GJ, Copeland TD, Oroszlan S, Snyderman R (1985) Inhibition of lymphocyte proliferation by a synthetic peptide homologous to retroviral envelope proteins. *Science* 230:453-455.
- Blaise S, Mangeney M, Heidmann T (2001) The envelope of Mason-Pfizer monkey virus has immunosuppressive properties. *J Gen Virol* 82:1597-1600.
- Mangeney M, Heidmann T (1998) Tumor cells expressing a retroviral envelope escape immune rejection in vivo. *Proc Natl Acad Sci USA* 95:14920-14925.
- Mangeney M, et al. (2007) Placental syncytins: Genetic disjunction between the fusogenic and immunosuppressive activity of retroviral envelope proteins. *Proc Natl Acad Sci USA* 104:20534-20539.
- Sitbon M, et al. (1990) Sequences in the U5-gag-pol region influence early and late pathogenic effects of Friend and Moloney murine leukemia viruses. *J Virol* 64:2135-2140.
- Renard M, et al. (2005) Crystal structure of a pivotal domain of human syncytin-2, a 40 million years old endogenous retrovirus fusogenic envelope gene captured by primates. *J Mol Biol* 352:1029-1034.
- Urisman A, et al. (2006) Identification of a novel Gammaretrovirus in prostate tumors of patients homozygous for R462Q RNASEL variant. *PLoS Pathog* 2:e25.
- Benlagha K, Kyin T, Beavis A, Teyton L, Bendelac A (2002) A thymic precursor to the NK T cell lineage. *Science* 296:553-555.
- Letvin NL, et al. (2007) No evidence for consistent virus-specific immunity in simian immunodeficiency virus-exposed, uninfected rhesus monkeys. *J Virol* 81:12368-12374.
- Mansfield K, et al. (2008) Vaccine protection by live, attenuated simian immunodeficiency virus in the absence of high-titer antibody responses and high-frequency cellular immune responses measurable in the periphery. *J Virol* 82:4135-4148.
- Chen W, Qin H, Chesebro B, Cheever MA (1996) Identification of a gag-encoded cytotoxic T-lymphocyte epitope from FBL-3 leukemia shared by Friend, Moloney, and Rauscher murine leukemia virus-induced tumors. *J Virol* 70:7773-7782.
- Iwashiro M, et al. (1993) Multiplicity of virus-encoded helper T-cell epitopes expressed on FBL-3 tumor cells. *J Virol* 67:4533-4542.
- Rouse BT, Sarangi PP, Suvas S (2006) Regulatory T cells in virus infections. *Immunol Rev* 212:272-286.
- Ralainirina N, et al. (2007) Control of NK cell functions by CD4+CD25+ regulatory T cells. *J Leukocyte Biol* 81:144-153.
- Robertson SJ, Messer RJ, Carmody AB, Hasenkrug KJ (2006) In vitro suppression of CD8+ T cell function by Friend virus-induced regulatory T cells. *J Immunol* 176:3342-3349.
- Dittmer U, et al. (2004) Functional impairment of CD8(+) T cells by regulatory T cells during persistent retroviral infection. *Immunity* 20:293-303.
- Iwashiro M, et al. (2001) Immunosuppression by CD4+ regulatory T cells induced by chronic retroviral infection. *Proc Natl Acad Sci USA* 98:9226-9230.
- Myers L, Messer RJ, Carmody AB, Hasenkrug KJ (2009) Tissue-specific abundance of regulatory T cells correlates with CD8+ T cell dysfunction and chronic retrovirus loads. *J Immunol* 183:1636-1643.
- Zelinskyy G, et al. (2005) CD8+ T-cell dysfunction due to cytolytic granule deficiency in persistent Friend retrovirus infection. *J Virol* 79:10619-10626.
- Zelinskyy G, Kraft AR, Schimmer S, Arndt T, Dittmer U (2006) Kinetics of CD8+ effector T cell responses and induced CD4+ regulatory T cell responses during Friend retrovirus infection. *Eur J Immunol* 36:2658-2670.
- Zelinskyy G, et al. (2009) The regulatory T-cell response during acute retroviral infection is locally defined and controls the magnitude and duration of the virus-specific cytotoxic T-cell response. *Blood* 114:3199-3207.
- He H, et al. (2004) Reduction of retrovirus-induced immunosuppression by in vivo modulation of T cells during acute infection. *J Virol* 78:11641-11647.
- Andrews DM, et al. (2005) Cross-talk between dendritic cells and natural killer cells in viral infection. *Mol Immunol* 42:547-555.
- Guernonprez P, Valladeau J, Zitvogel L, Théry C, Amigorena S (2002) Antigen presentation and T cell stimulation by dendritic cells. *Annu Rev Immunol* 20:621-667.
- Suzuki T, et al. (1995) Viral interleukin 10 (IL-10), the human herpes virus 4 cellular IL-10 homologue, induces local anergy to allogeneic and syngeneic tumors. *J Exp Med* 182:477-486.
- Blaise S, de Parseval N, Béné L, Heidmann T (2003) Genomewide screening for fusogenic human endogenous retrovirus envelopes identifies syncytin 2, a gene conserved on primate evolution. *Proc Natl Acad Sci USA* 100:13013-13018.
- Blaise S, Ruggieri A, Dewannieux M, Cosset FL, Heidmann T (2004) Identification of an envelope protein from the FRD family of human endogenous retroviruses (HERV-FRD) conferring infectivity and functional conservation among simians. *J Virol* 78:1050-1054.